Applied Catalysis B: Environmental 168-169 (2015) 195–202

Contents lists available at ScienceDirect

Applied Catalysis B: Environmental

journal homepage: www.elsevier.com/locate/apcatb

Deactivation and regeneration of a commercial SCR catalyst: Comparison with alkali metals and arsenic

Yue Peng[a,b], Junhua Li[a,*], Wenzhe Si[a], Jinming Luo[b], Yu Wang[a], Jie Fu[b], Xiang Li[a], John Crittenden[b,**], Jiming Hao[a]

[a] State Key Joint Laboratory of Environment Simulation and Pollution Control, School of Environment, Tsinghua University, Beijing 100084, China
[b] School of Civil and Environmental Engineering and the Brook Byers Institute for Sustainable Systems, Georgia Institute of Technology, 800 West Peachtree Street, Suite 400 F-H, Atlanta, GA 30332-0595, United States

ARTICLE INFO

Article history:
Received 13 October 2014
Received in revised form 1 December 2014
Accepted 2 December 2014
Available online 12 December 2014

Keywords:
SCR
DFT
Alkali
Arsenic
Regeneration

ABSTRACT

Deactivation of alkali metals and arsenic and regeneration methods are studied on commercial V_2O_5–WO_3/TiO_2 for the SCR reaction using experiments and DFT calculations. The poisoning of alkali metals is found to decrease the amount of Brønsted acid sites and the reducibility of active V^{5+} sites. Arsenic decreases the amount of Lewis acid sites and the stability of Brønsted acid sites and increases N_2O formation. After the catalysts are poisoned by both alkali metals and arsenic, the activity and N_2 selectivity are significantly suppressed. Diluted H_2SO_4 effectively removes alkali metals from the poisoned catalysts. Half of the amount of arsenic can be removed using a 4% H_2O_2 solution; however, some V_2O_5 and surface sulfates are also eliminated from the catalysts. The activity of the regenerated catalysts is almost recovered at high temperatures. From the DFT results on the V_2O_5/TiO_2 (0 0 1) plane, potassium and arsenic significantly alter the electronic structures of the V orbitals and broaden the band gap of the models. Interactions between potassium and arsenic are also found. Potassium covers the active sites of the models that are constructed by V_2O_5 and As_2O_5, which further decreases the number of acid sites. Potassium causes V and As orbitals to move to lower energies and inhibits the reactivity of the model.

1. Introduction

Pollutants are continuously emitted from the burning of fossil fuels, biomass and waste in power plants and waste incineration facilities. The emissions of NO_x, SO_x and NH_3 could cause environment acidification and haze formation in the atmosphere. The selective catalytic reduction (SCR) of NO_x with NH_3 is widely used for flue gas cleaning, and the most commonly used catalyst is vanadium on TiO_2 anatase, which works in the temperature range of 300–450 °C [1–5]. The catalytic convertor is often placed immediately after the combustion and before the electrostatic precipitator and flue gas desulfurization to take advantage of the heat from the hot exhaust gas [6,7]. However, major drawbacks of this arrangement are the facts that the monolith catalyst is exposed to high concentrations of SO_2 and alkali metals or heavy metals in the flow gas, which limits the working lifetime of the convertor. SO_2 has dual effects on the vanadia-based SCR catalyst depending on the temperatures. SO_2 does not inhibit or promote the SCR activity above 350 °C because of a formation of weakly reversibly sulfated and the formation of additional Brønsted acid sites. However, the SCR activity gradually decreases below 300 °C when ammonia bisulfate salts (ABS) are formed by SO_2 and H_2O in the flow gas. The ABS may cause surface fouling and/or pore clogging of the convertor and flue gas equipment [8–10].

Alkali metals in fly ash are a major concern from municipal solid-waste incineration plants and coal-fired plants, and arsenic is a serious poison for commercial SCR catalysts from stationary sources, where it is presented as As_2O_3 in the gas phase of power plants at concentrations between 1 μg/m^3 and 10 mg/m^3 [11,12]. The well-known mechanistic scheme is that the SCR catalyst follows a double-separated site, where the acid sites adsorb gaseous NH_3 and the redox sites activate the adsorbed NH_3 so that it can react with NO_x to form nitrogen [13,14]. Alkali metals are chemisorbed onto the active sites and form stable metal oxides. These species reduce the number of Brønsted acid sites and the catalyst reducibility by replacing the surface hydroxyls [12,15–21]. Arsenic (As) is deactivated because of the consumption of Lewis acid sites and the formation of unstable arsenic hydroxyls [22–24].

* Corresponding author. Tel.: +86 10 62771093; fax: +86 1 404 894 5676.
** Corresponding author. Tel.: +1 404 894 5676; fax: +1 404 894 5676.
E-mail addresses: lijunhua@tsinghua.edu.cn (J. Li), john.crittenden@ce.gatech.edu (J. Crittenden).

http://dx.doi.org/10.1016/j.apcatb.2014.12.005
0926-3373/

However, possible structures of the poisoned surfaces, interactions between alkali metals and As, and their effects on active sites must be elucidated.

Poisoned catalysts can be washed to prolong their working lifetime. Although hot-water washing is a good method to remove alkali metals on a ceria-based catalyst, it is less effective for vanadia-based catalysts [20]. Diluted H_2SO_4 has been shown to be more effective than water [25,26]; however, it does not effectively remove As. A considerable amount of arsenic oxides (mainly As_2O_5) may remain on the catalyst surface. Consequently, we must evaluate several regeneration methods for various poisoning events and compare these methods based on convenience and efficiency.

Two types of commercial V_2O_5–WO_3/TiO_2 catalysts were first compared. The sample with better SO_2 resistance was selected for the subsequent poisoning and regeneration studies. The effects of alkali metals and arsenic on the catalyst surface acidity and reducibility were investigated using TPD, DRIFTS spectra and TPR. The regeneration efficiency of diluted H_2SO_4 and H_2O_2 were determined based on the ICP results and catalytic-activity measurements. Density Functional Theory (DFT) calculations were used to determine the electronic structures between surface vanadium and the poisons.

2. Materials and methods

2.1. Catalyst poisoning and regeneration

Two types of commercial SCR catalysts were obtained from a coal-fired power plant in southwest China, which were defined as samples 1# and 2#, where the V_2O_5 loading was approximately 1 wt.%. All of the catalysts were crushed and sieved within 40–60 meshes for activity measurements and with more than 60 meshes for chemical characterizations. After evaluating the SCR performance of the catalysts, we selected sample 2# for the subsequent poisoning and regeneration studies.

Alkali metals were added to the catalysts by wet-impregnating different concentrations of KNO_3 or $NaNO_3$ solutions. The catalyst of the alkali metal loading was defined as pK*x* or pNa*x*, where *x* denotes the weight percent of the alkali metals. Arsenic metal was added to the catalysts using As_2O_3 steam (350 °C, 3% H_2O/N_2 in the tube furnace) and by exposing the catalysts to an O_2-rich condition (3%) for 10 h at 370 °C. The catalyst loading of arsenic was 0.48 wt.%, and the sample is denoted as pAs.

The samples that were co-poisoned with alkali metals and arsenic were obtained by poisoning them first with arsenic (0.48 wt.%) and subsequently with alkali metals. The sample is denoted as pAsK*x*, where *x* denotes the loading of alkali metals. For pAsK*x* poisoned catalysts, we first removed alkali metals using diluted H_2SO_4, which is called the deK process. Second, we removed arsenic using an aqueous solution of H_2O_2, which is called the deAs process. We regenerated these catalysts as pAsK0.25, pAsK0.5 and pAsK1.

2.2. SCR activity measurement

The SCR reactions were performed in a fixed-bed quartz reactor using 200 mg of catalysts for the catalyst selection and 100 mg for the poisoning studies. The feed gas mixture contained 500 ppm NO, 500 ppm NH_3, 3% O_2, 5% H_2O and 200 ppm SO_2 (when used), and the balance was N_2. The gas concentrations of NH_3, N_2O, NO, NO_2, SO_2 (ppm) and water vapor (%) were continually monitored using an FTIR spectrometer (GASMET FTIR DX-4000). The test temperature was 150–450 °C. The concentrations were collected when the reaction reached a steady state after 30 min at each temperature and after 60 min for the water-containing experiments, where 5% steam was introduced into the gas flow.

The NO_x (NO and NO_2) conversion is as follows:

$$NO_x \text{ conversion} = \left(1 - \frac{NO_x(\text{out})}{NO(\text{in})}\right) \times 100\%$$

2.3. Catalyst characterization

The BET surface area was calculated using a Micromeritics ASAP 2020 apparatus. The elemental content was measured using an ICP-AES and an IRIS Intrepid II XSP apparatus (Thermo Fisher Scientific Inc.). The DRIFTS spectra were recorded using a Fourier transform infrared spectrometer (FTIR, Nicolet NEXUS 870), which was equipped with a Harrick IR cell, and an MCT detector, which was cooled by liquid N_2. The catalyst was first heated to 350 °C under N_2 at a total flow rate of 100 mL/min for 60 min to remove the adsorbed impurities. The background spectrum was collected in a flowing N_2 atmosphere, and the background spectra were subtracted from the sample spectra. The IR spectra were recorded by accumulating 32 scans, and the resolution was 4 cm^{-1}. The temperature programmed reduction (TPR) of H_2 was performed on a chemisorption analyzer (ChemiSorb 2720 TPx) under 10% H_2/Ar gas flow (50 mL/min) at a rate of 10 °C/min up to 900 °C. The temperature programmed desorption (TPD) of NH_3 was performed in a fixed-bed quartz reactor. Before the test, each sample (100 mg) was pretreated in N_2 (200 mL/min) gas at 350 °C. The sample was then purged with NH_3 (500 ppm) at room temperature. After isothermal desorption under an N_2 gas flow (200 mL/min) at 100 °C, the temperature was increased to 600 °C at a rate of 10 °C/min. The NH_3 concentrations were monitored using MultiGas TM 2030.

2.4. DFT calculations

All structural optimizations were based on DFT and performed using the Material Studio 5.5 software with plane-wave basis sets [27]. A plane-wave energy cutoff of 400 eV was used in all cases. The generalized gradient approximation plus Hubbard model (GGA + U) according to Perdew, Burke and Ernzerhof (PBE) was used, where the value of U was set to 3.5 for titanium [28–31]. The Monkhorst-Pack division scheme was selected to generate a set of k-point within the Brillouin zone. For the TiO_2 anatase support, although the (1 0 1) plane is thermodynamically more stable, the (1 0 0) and (0 0 1) planes are found in industrial TiO_2 powers, and previous studies also proposed that the (0 0 1) plane plays an important role during the catalytic reaction [32,33]. The TiO_2 (0 0 1) plane was constructed by cutting the TiO_2 anatase and a (3 × 3) supercell of the slab model. A vacuum gap of 15 Å was used to separate subsequent slabs ($Ti_{36}O_{72}$). The slab thickness was optimized according to previous TiO_2 (0 0 1) slab results [34–36], where a 3-layer slab model with the bottom layer fixed to the bulk parameters was sufficient and had a low computing cost. For the surface relaxation, no symmetry was used, and a dipole correction was included.

3. Results and discussion

3.1. Catalyst selection

Fig. 1(a) shows the SCR activity of commercial V_2O_5–WO_3/TiO_2 (samples 1# and 2#) under GHSV of 60,000 h^{-1}. Sample 2# exhibits better activity than sample 1# below 350 °C. The NO_x conversions of the catalysts were similar above 350 °C, and both decreased at higher temperatures. This phenomenon could occur because of the oxidation of NH_3 with excess O_2 in the flue gas [6]. When 200 ppm

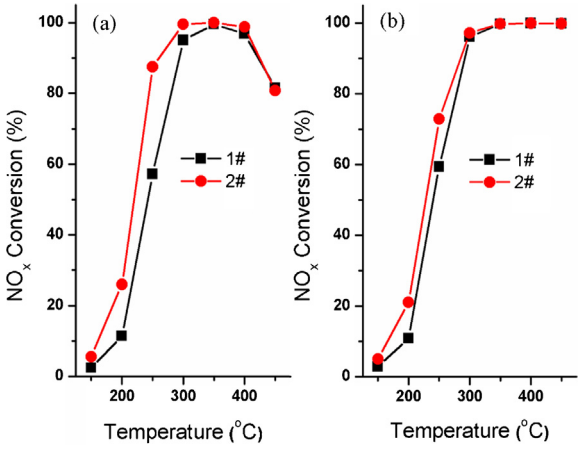

Fig. 1. (a) SCR activity of commercial V_2O_5–WO_3/TiO_2 catalysts; (b) SCR activity of commercial catalysts in the presence of 200 ppm SO_2. Reaction conditions for (a) and (b): [NO] = [NH_3] = 500 ppm, [O_2] = 3%, total flow rate = 200 mL/min, GHSV = 60,000 h^{-1}.

SO_2 was introduced (Fig. 1(b)), sample 2# yielded higher activity than sample 1#, and the activities of both catalysts dramatically decreased to 300 °C. The decrease is mainly caused by the coverage of ammonia bisulfate salts (ABS) on the catalyst surface [7]. The activity in the presence of SO_2 showed no considerable suppression above 300 °C. These results can be attributed to the formation of strong Brønsted acid sites or the transformation of isolated vanadyl species into polymeric species by occupying parts of the free carrier materials at high temperatures [6]. Sample 2# was selected for the following catalyst poisoning and regenerating study and denoted as "fresh".

3.2. Poisoned by alkali metals and arsenic

Fig. 2 shows the NO_x conversions and N_2O formations of fresh and poisoned catalysts with alkali metals and arsenic under a GHSV of 120,000 h^{-1}. The activity was suppressed by the poisons, and the deactivation extent was directly related to the poison loading. When the amount of potassium was larger than 0.5 wt.%, only 20% of the NO_x conversion was obtained at 400 °C. Fig. 2(b) shows the N_2O concentrations of the catalysts during the SCR measurement. As known, N_2O is an important atmospheric pollutant because N_2O can cause increased global warming and stratospheric ozone depletion [37]. The fresh catalyst only generated approximately 11 ppm N_2O at 450 °C, whereas the poisoned samples produced more than 30 ppm N_2O under the same GHSV. N_2O was not considerably promoted with increased potassium loadings, i.e., most N_2O may be present because of the arsenic oxides.

The effects of potassium and sodium on arsenic-poisoned catalysts were also examined (Fig. 2(c) and (d)). pAsNa1 exhibited more severe poisoning behaviors than pAsK1 above 350 °C, which indicated that for an equal mass loading of K and Na of 1 wt.%, there is approximately 70% more sodium on the catalyst than potassium [18]. Commonly, potassium leads to more deactivation than sodium at the same molar concentration because of its more potent neutralizing property, and the chemical poisoning extent for alkali/alkaline earth metals is proposed: K>Na>Ca>Mg [18,38,39]. To confirm this hypothesis, the catalyst pAsK0.5Na0.5 was also prepared, and its activity profile was precisely between those of pAsNa1 and pAsK1. N_2O was slightly restrained by increasing the ratio of sodium oxides (Fig. 2(d)). Therefore, neither potassium nor sodium provides additional N_2O at high temperatures.

The XRD patterns of the poisoned catalysts are shown in Fig. S1. Increasing the potassium or varying the sodium ratio does not change the peak positions or intensities. Alkali metals and arsenic

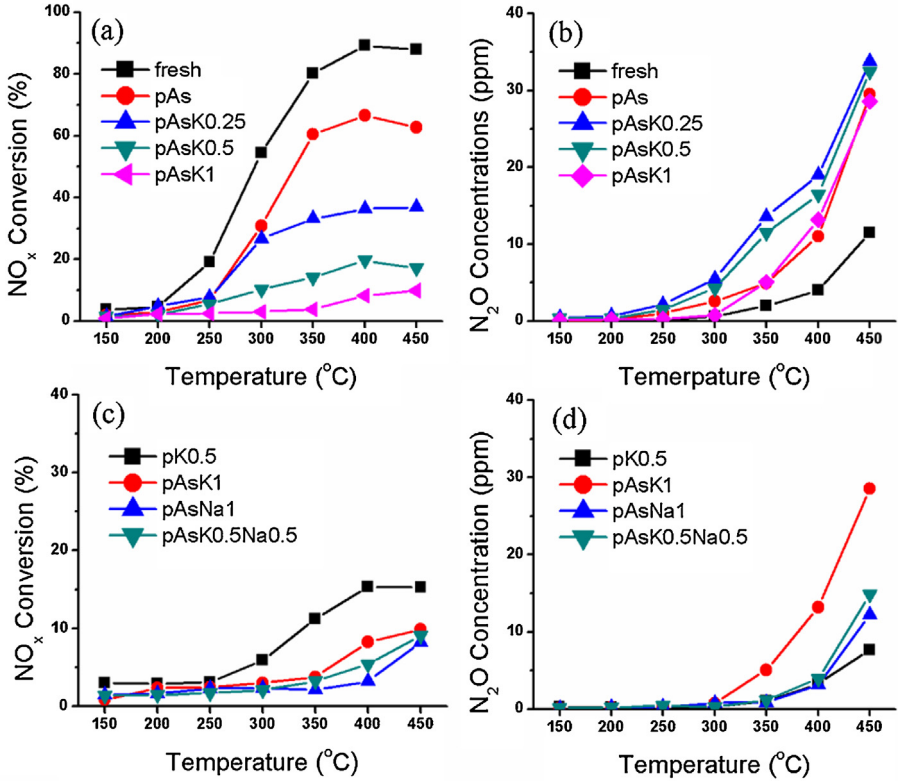

Fig. 2. (a) NO_x conversion and (b) N_2O formation of fresh and poisoned catalysts with arsenic and potassium; (c) NO_x conversion and (d) N_2O formation of the catalysts poisoned with arsenic and potassium and/or sodium. Reaction condition: [NO] = [NH_3] = 500 ppm, [O_2] = 3%, total flow rate = 200 mL/min, GHSV = 120,000 h^{-1}.

Table 1
Comparison on the BET surface area and total surface acidity of fresh, poisoned and regenerated catalysts.

	Fresh	pK0.5	pAs	pAsK1	deK	deAs
Surface area (m^2/g)	50.99	48.83	49.79	51.15	60.10	58.41
Total acidity (mmol/g)	0.537	0.249	0.465	0.074	0.480	0.554
Total acidity (μmol/m^2)	10.53	5.10	9.34	1.45	7.99	9.48

do not change the phase structures of the catalysts at certain poison contents. The BET surface areas of fresh, pK0.5, pAs, and pAsK1 catalysts are listed in Table 1. The BET surface area does not critically decrease after poisoning at certain loadings.

3.3. Regeneration of the poisoned catalysts

Different concentrations of diluted H_2SO_4 and H_2O_2 solutions were used to eliminate potassium and arsenic, respectively (Fig. S2). When the diluted H_2SO_4 solutions were higher than 0.2 M, the potassium content was nearly identical to that of the fresh catalyst. When the H_2O_2 solutions were higher than 4 M, the arsenic content remained constant; however, the vanadium loadings of the catalyst began to decline. Therefore, 0.2 M H_2SO_4 and 4 M H_2O_2 were selected for the deK and deAs processes, respectively. Fig. 3 shows the element contents of K, As, S (sulfates in catalyst) and V after the H_2SO_4 and H_2O_2 treatment for the pAsK0.25, pAsK0.5 and pAsK1 catalysts; the main differences among the samples are the potassium loadings. More than 90% of the potassium amount was eliminated from the catalysts. However, the surface V, As and S also decreased with 0.2 M H_2SO_4 to some extents. After the following deAs process, the As content diminished, and both S and V also considerably decreased. Accordingly, more S and V decreased during the deAs process than during in the deK process. A previous study also proposed that the decrease of S considerably suppressed the catalyst activity, particularly within its working temperatures [10]. The amount of V gradually decreased, and nearly 10% of V was lost after the deAs process. The results indicate that the active components, such as vanadia and SO_4^{2-}, must be added after the washing procedure. The BET surface areas of the regenerated catalysts are also listed in Table 1. The values of the surface areas did not considerably increase after the washing.

Fig. 4 presents the SCR performance of the catalysts after deK and deAs. The NO conversions of the three catalysts (pAsK0.25, pAsK0.5 and pAsK1) significantly improved after the deK process. The activities of pAsK0.25 were nearly identical to those of the fresh catalysts above 350 °C. Although these three catalysts have less N_2O formation than the corresponding poisoned catalyst, they remained higher than the fresh catalyst. Accordingly, N_2O originates from arsenic poisoning instead of alkali metals. Furthermore, the activity of pAsK0.25 after the deAs process increased at low temperatures, and the activity at high temperature can be preserved compared with pAsK0.25 after the deK process. Furthermore, the activities of pAsK0.5 and pAsK1 in Fig. 4(c) were slightly lower than those of the corresponding catalysts after the deK process because of the combined effect of residual K (negative factor), loss of V and S (negative factor) and elimination of As (positive factor). The loss of surface arsenic and vanadia decreased N_2O after the deAs process at 450 °C (Fig. 4(d)). The excess vanadia in the SCR catalyst are highly active on N_2O formation above 350 °C and the lower V and As loadings correspond to the lower N_2O concentrations.

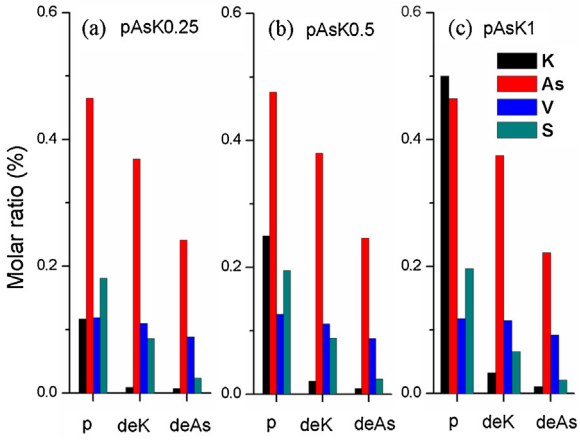

Fig. 3. ICP results of the K, V, S and As contents on the poisoned catalysts: (a) pAsK0.25, (b) pAsK0.5 and (c) pAsK1 after washing in 0.2 M H_2SO_4 (deK process) and 4 M H_2O_2 (deAs process). Wash time = 30 min, and vol.% of catalyst to solution = 1:5.

3.4. H_2-TPR and NH_3-TPD results

As previously discussed, the surface acidity and reducibility are the most critical properties of vanadia-based SCR catalysts. It is necessary to study the effect of alkali metals and arsenic on these two properties. Fig. 5(a) presents the H_2-TPR profiles of fresh and poisoned catalysts. Two peaks can be obtained on the fresh sample: the low-temperature peak (480 °C) can be assigned to the reduction of V^{5+} to V^{3+}, and the high-temperature peak (790 °C) can be assigned to the reduction of W^{6+} to W^0 [40,41]. The low-temperature peak shifts higher to 590 °C and the high-temperature peak shifts lower to approximately 770 °C for pK0.5. Doping potassium on the fresh catalyst may suppress the reducibility of vanadia species, which can suppress the catalyst activity. The reduction peak of vanadia becomes larger and shifts to lower temperatures (435 °C) for pAs, which suggests that arsenic enhances the catalyst reducibility. For the pAsK0.5 catalyst, the reduction peak of vanadia is between 438 and 600 °C (572 °C), and the reduction peak of W^{6+} appears at the

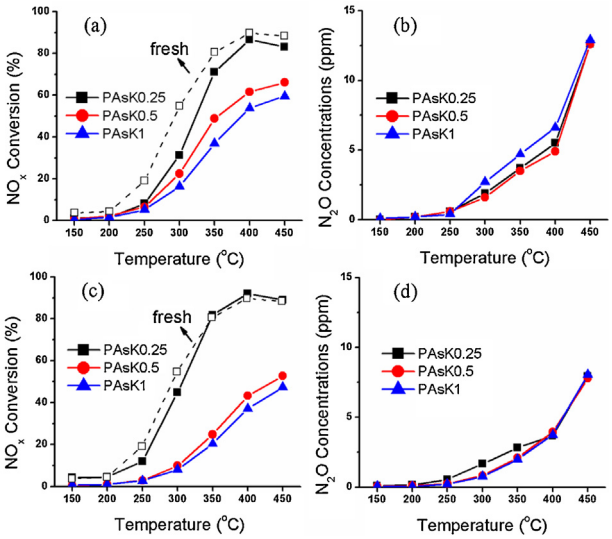

Fig. 4. (a) NO_x conversion and (b) N_2O formation of poisoned catalysts after the deK process; (c) NO_x conversion and (d) N_2O formation of poisoned catalysts after the deAs process. The dashed lines are the NO conversion of the fresh catalyst. Reaction conditions: [NO] = [NH_3] = 500 ppm; [O_2] = 3%; total flow rate = 200 mL/min; GHSV = 120,000 h^{-1}.

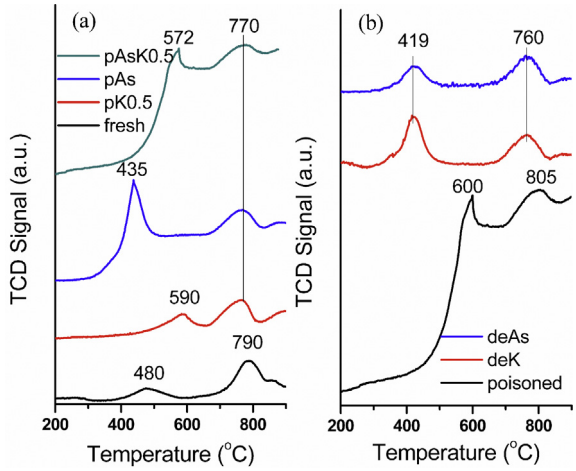

Fig. 5. H_2-TPR profiles of (a) fresh and poisoned catalysts with potassium and arsenic and (b) poisoned and regenerated pAsK1 catalysts at 200–900 °C. Reaction conditions: [H_2] = 10%; total flow rate = 50 mL/min.

identical position as those in pK0.5 and pAs. These results indicate that the alkali atoms suppress the reducibility of vanadia, arsenic improves their reducibility, and arsenic shows less effect on WO_3. Fig. 5(b) presents the H_2-TPR profiles of pAsK1 and the corresponding regenerated catalysts. The reduction peak of V^{5+} moves to a lower temperature (419 °C), and the total profiles are similar to those of pAs for the catalyst after the deK process., The peak positions of V^{5+} or W^{6+} are nearly unchanged, but the reduction peak slightly broadens and is similar to the shape of the fresh catalyst at 480 °C after the deAs process. The results indicate that the deK process can remove most alkali metals and some of the surface arsenic, which is consistent with the ICP results. Furthermore, the reduction peaks of deK and deAs are also lower than those of the fresh catalyst, which may be responsible for the decrease of amount of surface sulfates after the regeneration processes.

Fig. 6(a) shows the NH_3-TPD profiles of fresh and poisoned catalysts, and the total acidity of the catalysts is listed in Table 1. The total acidity of the fresh catalyst significantly decreases after poisoning by potassium and arsenic, both per sample mass and per surface area. The main desorption peak (245 °C) of pK0.5 slightly moves to a lower temperature (270 °C) compared to the fresh catalyst and pAs. The relatively high temperature shoulder (380 °C) decreases for the poisoned catalysts. Potassium may determine

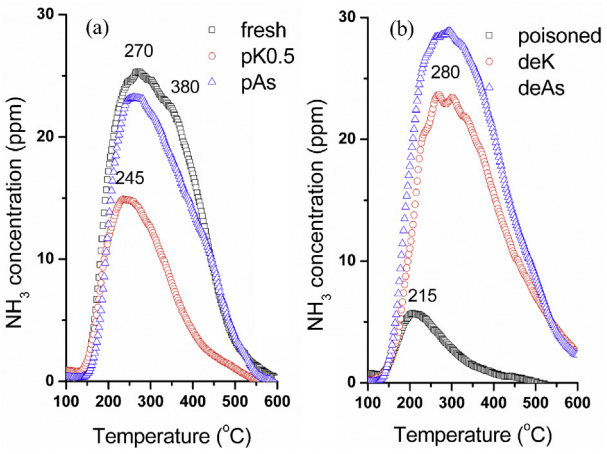

Fig. 6. NH_3-TPD profiles of (a) fresh and poisoned catalysts with potassium and arsenic and (b) poisoned and regenerated pAsK1 catalysts in the temperature range of 100–600 °C. Reaction condition: total flow rate = 200 mL/min.

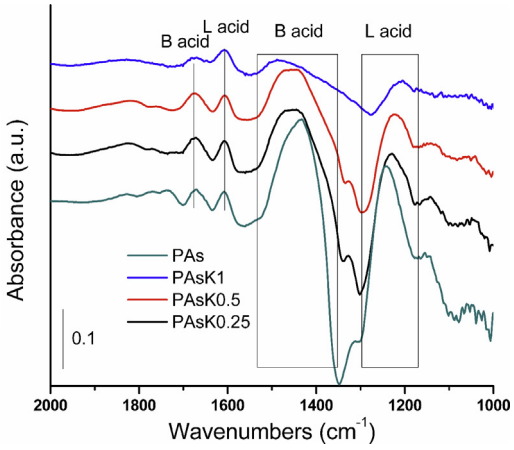

Fig. 7. In situ IR spectra of poisoned catalysts with potassium and arsenic at 50 °C.

both the amount and strength of the surface acid sites, whereas arsenic only shows a moderate effect on the surface acid sites. Fig. 6(b) shows the NH_3-TPD profiles of the poisoned and regenerated pAsK1 catalysts. The amount of surface acid sites significantly improves even during the deK process and the catalyst yields more NH_3 desorption after the deAs process. However, the total acidity per surface area after the deAs process (9.48 μmol/m^2) remains less than that of the fresh catalyst possibly because of the effect of the remaining arsenic on the catalyst surface. The main peak of pAsK1 (215 °C) moves to a higher temperature region, which suggests that the strong acid sites reappear after washing. The results are consistent with the SCR performance and ICP.

3.5. Types and strength of the acid sites

Based on our previous studies, alkali metals mainly occupy Brønsted acid sites; whereas arsenic consumes Lewis acid sites and forms weak, inactive Brønsted acid sites [19,20]. With respect to the investigation of acidity types, DRIFTS spectra were used on the NH_3 adsorption/desorption in the range of 50 to 350 °C. Fig. 7 presents the spectra of the catalysts that were poisoned with both potassium and arsenic at 50 °C. The broad band within 1150–1300 cm^{-1} as the $\delta_s(NH_3)$ mode and the peak at 1603 cm^{-1} as the $\delta_{as}(NH_3)$ mode can be attributed to Lewis acid sites; the broad band within 1390–1480 cm^{-1} as the $\delta_{as}(NH_4^+)$ mode and the peak at 1670 cm^{-1} as the $\delta_s(NH_4^+)$ mode can be attributed to Brønsted acid sites [42–46]. With increased potassium loading, the intensities of the Brønsted acid sites significantly decrease, whereas the intensities of the Lewis acid sites (1603 cm^{-1}) appear to be less affected. However, the band that is attributed to Lewis acid sites before 1300 cm^{-1} weakens for the pAsK1 sample possibly because of the interactions between a considerable amount of surface As and K.

Commonly, As_2O_3 is oxidized to As_2O_5 and diffuses into the catalyst lattice [47]. As and K may bond to both active (amorphous V_2O_5) and non-active sites (TiO_2 support), whereas K_2O is only adsorbed onto active sites [48,11]. DRIFTS of NH_3 desorption were used for pAsK0.25 and pAsK1 (arsenic loading are same) to study the role of potassium and arsenic (Fig. 8). The intensity of the peak at 1670 cm^{-1} significantly decreases with increased potassium loadings. When the temperature is increase to 150 °C, a large Brønsted acidity peak remains. The peak at 1603 cm^{-1} for pAsK0.25 shows a similar intensity to that for pAsK1 at 50 °C; however, this peak of pAsK1 quickly weakens with an increased temperature. Nearly all of the Brønsted acid sites (1603 cm^{-1}) are lost on pAsK1, whereas a small but detectable peak for Lewis acid sites remain observed at 250 °C. This result suggests that the amount of Brønsted acid sites is significantly suppressed on the poisoned catalyst, and the

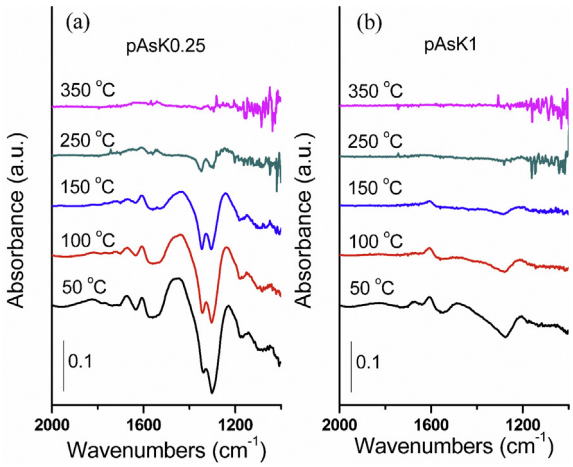

Fig. 8. NH_3 desorption performed on in situ IR spectra over (a) pAsK0.25 and (b) pAsK1 up to 350 °C.

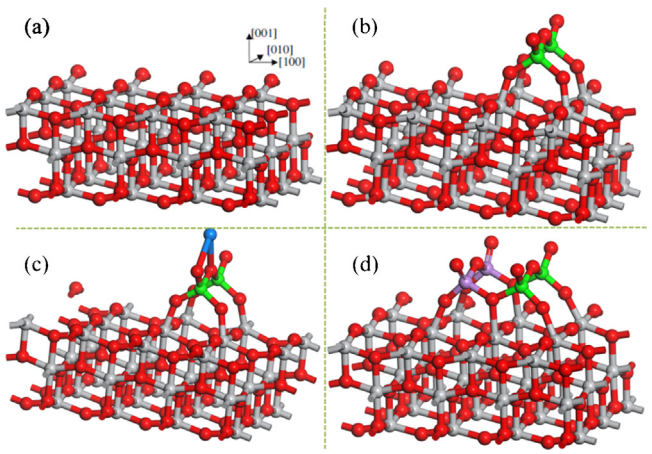

Fig. 10. Optimized structures of the (a) TiO_2 (0 0 1) plane and (b) V/Ti, (c) K–V/Ti and (d) As–V/Ti models. Gray, red, green, blue and violet balls are titanium, oxygen, vanadium, potassium and arsenic, respectively.

presence of potassium affects the quantity and strength of the Lewis acid sites that are formed by arsenic. In other words, there may be a further suppression of surface acidity when potassium and arsenic are both present.

Fig. 9 shows the DRIFTS spectra for NH_3 desorption, pK0.5 and pAsK0.5 in the temperature range of 50–350 °C. The number of Lewis acid sites (1607 cm^{-1}) decreases with increased arsenic loading, and the broad band of pK0.5 centered at 1200 cm^{-1} also narrows compared to that of pAsK0.5. When the temperature is 350 °C, partial Lewis acid sites remain observed on pK0.5, whereas nearly all Lewis acid sites disappear at 350 °C, and the quantity of Brønsted acid sites significantly increases on pAsK0.5. These new acid sites adsorb the gaseous NH_3 as NH_4^+ but show less promotion on the SCR activity because of the weakly bondage to the surface. With increased temperatures, the Brønsted acid sites of pK0.5 and pAsK0.5 disappear at 250 °C, which indicates the low thermal stability of Brønsted acid sites at higher temperatures. Furthermore, a weak peak at 1538 cm^{-1} occurs for pAsK0.5. This peak is assigned to the vibrations of NH_2 species from the NH_3 oxidation with the lattice oxygen and indicates the redox property of the catalyst surface [49,50]. More NH_2 formation on the surface leads to more N_2O at high temperatures. The results are consistent with the N_2O origin and trends. Fig. S3 shows the DRIFTS spectra of the poisoned catalysts after the deK and deAs processes of pAsK0.25, pAsK0.5 and pAsK1. The loss of Brønsted acid sites in quantity may be attributed to the reduction of amount of surface sulfates and active sites V_2O_5, whereas the loss of Lewis acid sites may be attributed to the decrease of V_2O_5. V_2O_5 provides both quantities of Lewis and Brønsted acid sites, and the adsorbed NH_3 on both Lewis and Brønsted acid sites are active for the SCR reaction [6]. After the washing processes with diluted H_2SO_4 and H_2O_2, alkali metals can be effectively eliminated; however, half of the arsenic remains on the catalyst. The SCR performance of the regenerated pAsK1 sample at 370 °C under 200 ppm SO_2, 5% H_2O and high GHSV shows that the NO conversion is preserved between 50 and 60%, and the N_2O formation is less than 3 ppm (Fig. S4).

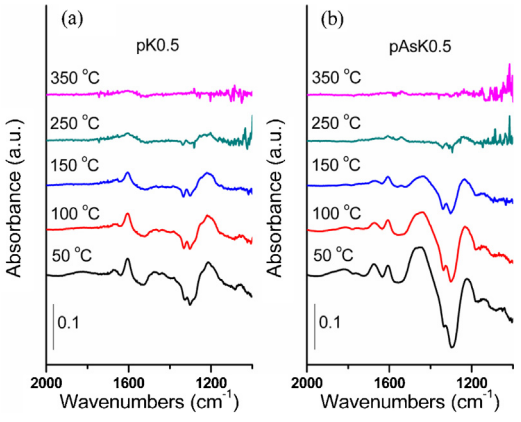

Fig. 9. NH_3 desorption performed on in situ IR spectra over (a) pK0.5 and (b) pAsK0.5 up to 350 °C.

3.6. Interactions between poisons and V_2O_5/TiO_2

Sub monolayer models were selected to investigate the interaction of vanadia and poisons because the commercial SCR catalyst had a low vanadia loading (<1 wt.%) on the catalyst. For this low-loading system, the vanadia dimer was modeled as having a 4-fold coordination with two adjacent vanadium sites in a similar configuration to those found on the (0 1 0) plane of the V_2O_5 bulk (Fig. 10). The bond lengths of V=O and V—O—V are 1.62 and 1.80 Å, respectively, and the V_2O_5 cluster is 1.89 Å higher than the TiO_2 (0 0 1) plane, which shows similar results as previous DFT studies [36,51]. Potassium and arsenic atoms were doped on the modeled surfaces as K_2O and As_2O_5 according to the previous work and experimental results [12,22]. From the configurations of the poisoned models, it is suggested that the poisons may cover the active sites of the models from the top and sides of the vanadium atoms. The distances of potassium and arsenic to the nearest vanadium were 3.31 and 3.32 Å, respectively. Fig. 11(a) shows the projected density of the states (PDOS) of V 3d orbitals for the V/Ti, K–V/Ti and As–V/Ti models. Both the top of the valence band and the bottom of the conduction band of the V 3d orbitals changed considerably when the V/Ti model was doped by potassium and arsenic atoms. The band gap size was K–V/Ti>V/Ti>As–V/Ti, and the sequence of the distances from the top of valence band to the Fermi level was K–V/Ti>As–V/Ti>V/Ti. This result suggests that the reactivity of vanadium atom on the V/Ti model decreases with increased potassium and arsenic poisoning. To elucidate the effect of the poisons on the active sites of vanadia (V=O bond and V—O—V bond), the PDOS of O 2p in both the V=O and V—O—V groups of V/Ti and the poisoned V/Ti were investigated (Fig. 11(b)). The top of the valence band of O 2p in V/Ti moved to a lower energy after potassium or arsenic poisoning. Combined with the results of the V 3d orbitals, one can conclude that the reactivity of both V=O and V—O—V groups of the V/Ti models decreases because of the bondage of As and K atoms to the surface active oxygen.

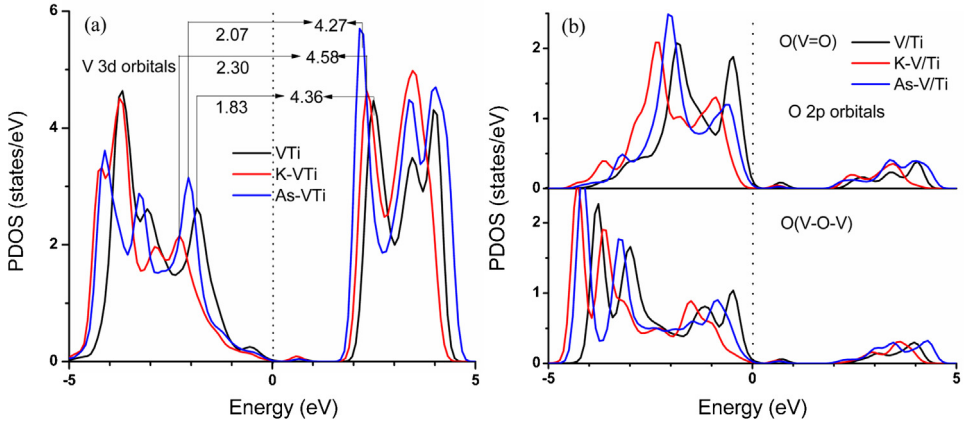

Fig. 11. PDOS of (a) V 3d and (b) O 2p of the V/Ti, K–V/Ti and As–V/Ti models.

Another important topic is whether there is an interaction between potassium and arsenic atoms, which further deactivates the V_2O_5-based catalyst. Both potassium and arsenic atoms on the V/Ti model were modeled, whereas potassium was doped on the slab of V_2O_5, and the As_2O_5 cluster was doped on the TiO_2 (0 0 1) plane (Fig. 12, TiO_2 slabs are not shown). Regardless of the positions of potassium above the vanadium-arsenic cluster, it tends to occupy the space above the active sites instead of tightly bonding to a surface oxygen atom. Therefore, the acid sites are blocked and strictly unavailable on both vanadium and arsenic sites, which can account for the decrease of Lewis and Brønsted acid sites on the pAsK1 sample. The PDOSs of the V, K and As orbitals are also shown. The conduction band is constructed with V orbitals and partial As orbitals. Most of the K orbitals occur in the middle of the valence band (−12.5 eV), which indicates that potassium was less active. Furthermore, the As orbitals considerably move to low energy when potassium is doped on the top of the surface. The results suggest that the interactions between potassium and arsenic increase the stability of the catalytic surface and decrease the catalyst activity.

In summary, the DFT results imply that potassium and arsenic occupy Brønsted acid and Lewis acid sites, respectively, and both of them decrease the reactivity of the V/Ti models. There are interactions between potassium and arsenic, which can decrease the reactivity of the active sites.

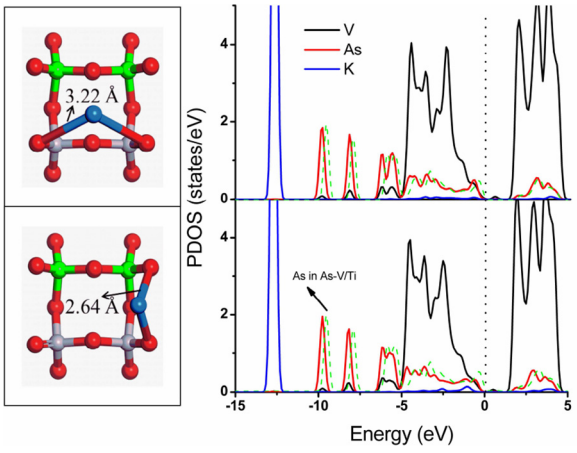

Fig. 12. Optimized structures and PDOS of surface V, As and K atoms for the K, As co-doped V/Ti models. The green dashed lines are the PDOS of As orbitals in the As–V/Ti model.

4. Conclusion

We focus on the chemical poisoning mechanism of alkali metals and arsenic on commercial SCR catalysts. Alkali metals decrease the number of Brønsted acid sites and the reducibility of active V^{5+} sites, which leads to significant catalyst poisoning, but alkali metals show less promotion for N_2O formation. Arsenic decreases the number of Lewis acid sites and the strength of Brønsted acid sites. Furthermore, As_2O_5 on the surface considerably increases the N_2O amount at high temperatures. The catalyst activity is more reduced when both K and As are on the surface than when the catalyst s are on the surface by themselves.

Washing the catalyst with diluted H_2SO_4 solutions is an effective method to reduce the amount of alkali metals. However, parts of the vanadium and surface sulfate are also removed when arsenic is reduced using H_2O_2 solutions. The regenerated catalysts shows good SCR activity at high temperatures, but the activity must be improved at low temperature.

By calculating the electronic structures of poisons doped on the V/Ti (0 0 1) plane models, potassium and arsenic significantly affect the V 3d orbitals and broaden the band gap of the poisoned catalysts. Potassium covers the active sites of the model that is constructed with V_2O_5 and As_2O_5 clusters, which further decreases the number of acid sites. Moreover, potassium causes the V and As orbitals to move to lower energies, which stabilizes the catalytic surfaces and decreases the catalyst reactivity.

Conflict of interest

The authors declare no competing financial interest.

Acknowledgments

The authors gratefully acknowledge the financial supports from National Natural Science Foundation of China (21407088), and National High-Tech Research and the Development (863) Program of China (2013AA065401) and the International Postdoctoral Exchange Fellowship Program of China (20130032). The authors appreciate support from the Brook Byers Institute for Sustainable Systems, Hightower Chair and Georgia Research Alliance at Georgia Institute of Technology. The author would also like to thank Prof. Weixue Li and Dr. Chuanqi Huang of Dalian Institute of Chemical Physics in China.

Appendix A. Supplementary data

Supplementary data associated with this article can be found, in the online version, at http://dx.doi.org/10.1016/j.apcatb.2014.12.005.

References

[1] G. Ramis, F. Bregani, Appl. Catal. 64 (1990) 259–278.
[2] V. Marshneva, J. Catal. 155 (1995) 171–183.
[3] P. Ciambelli, M. Fortuna, D. Sannino, A. Baldacci, Catal. Today 29 (1996) 161–164.
[4] G. Ramis, L. Yi, Catal. Today 28 (1996) 373–380.
[5] L. Lietti, I. Nova, P. Forzatti, Top. Catal. 11–12 (2000) 111–122.
[6] G. Busca, L. Lietti, G. Ramis, F. Berti, Appl. Catal. B: Environ. 18 (1998) 1–36.
[7] Z. Liu, S. Woo, Catal. Rev. 48 (2006) 43–89.
[8] J. Dunn, P. Koppula, H. Stenger, I. Wachs, Appl. Catal. B: Environ. 19 (1998) 103–117.
[9] Z. Huang, Z. Zhu, Z. Liu, Appl. Catal. B: Environ. 39 (2002) 361–368.
[10] M. Kobayashi, M. Hagi, Appl. Catal. B: Environ. 63 (2006) 104–113.
[11] C. Senior, D. Lignell, A. Sarofim, A. Mehta, Combust. Flame 147 (2006) 209–221.
[12] L. Lisi, G. Lasorella, S. Malloggi, G. Russo, Appl. Catal. B: Environ. 50 (2004) 251–258.
[13] N. Topsoe, Science 265 (1994) 1217–1219.
[14] N. Topsoe, J. Catal. 151 (1995) 226–240.
[15] L. Lietti, P. Forzatti, G. Ramis, G. Busca, F. Bregani, Appl. Catal. B: Environ. 3 (1993) 13–35.
[16] H. Kamata, K. Takahashi, C. Odenbrand, J. Mol. Catal. A: Chem. 139 (1999) 189–198.
[17] O. Kröcher, M. Elsener, Appl. Catal. B: Environ. 77 (2008) 215–227.
[18] L. Chen, J. Li, M. Ge, Chem. Eng. J. 170 (2011) 531–537.
[19] Y. Peng, J. Li, L. Chen, J. Chen, J. Han, H. Zhang, W. Han, Environ. Sci. Technol. 46 (2012) 2864–2869.
[20] Y. Peng, J. Li, W. Shi, J. Xu, J. Hao, Environ. Sci. Technol. 46 (2012) 12623–12629.
[21] Y. Peng, J. Li, X. Huang, X. Li, W. Su, X. Sun, D. Wang, J. Hao, Environ. Sci. Technol. 48 (2014) 4515–4520.
[22] E. Hums, Res. Chem. Intermed. 19 (1993) 419–441.
[23] F. Lange, H. Schmelz, H. Knözinger, Appl. Catal. B: Environ. 8 (1996) 245–265.
[24] Z. Wei, S. Zhang, Z. Pan, Y. Liu, Appl. Surf. Sci. 258 (2011) 1192–1198.
[25] R. Khodayari, C. Odenbrand, Appl. Catal. B: Environ. 33 (2001) 277–291.
[26] R. Khodayari, C. Odenbrand, Appl. Catal. B: Environ. 30 (2001) 87–99.
[27] A. Becke, Phys. Rev. A 38 (1988) 3098–3100.
[28] J. Perdew, K. Burke, M. Ernzerhof, Phys. Rev. Lett. 77 (1996) 3865–3868.
[29] B. Delley, Phys. Rev. B 66 (2002) 155125.
[30] J. Graciani, J. Plata, J. Sanz, P. Liu, J. Rodriguez, J. Chem. Phys. 132 (2010) 104703.
[31] M. Ganduglia-Pirovano, A. Hofmann, J. Sauer, Surf. Sci. Rep. 62 (2007) 219–270.
[32] M. Calatayud, B. Mguig, C. Minot, Theor. Chem. Acc. 114 (2005) 29–37.
[33] M. Calatayud, C. Minot, Top. Catal. 41 (2006) 17–26.
[34] A. Vittadini, M. Casarin, A. Selloni, Theor. Chem. Acc. 117 (2006) 663–671.
[35] P. Hejduk, M. Witko, K. Hermann, Top. Catal. 52 (2009) 1105–1115.
[36] A. Suarez Negreira, J. Wilcox, J. Phys. Chem. C 117 (2012) 1761–1772.
[37] S. Yang, S. Xiong, Y. Liao, X. Xiao, F. Qi, Y. Peng, Y. Fu, W. Shan, J. Li, Environ. Sci. Technol. 48 (2014) 10354–10362.
[38] Q. Wan, L. Duan, J. Li, L. Chen, K. He, J. Hao, Catal. Today 175 (2011) 189–195.
[39] X. Du, X. Gao, R. Qu, P. Ji, Z. Luo, K. Cen, ChemCatChem 4 (2012) 2075–2081.
[40] C. Wang, S. Yang, H. Chang, Y. Peng, J. Li, Chem. Eng. J. 225 (2013) 520–527.
[41] S. Yang, C. Wang, J. Chen, Y. Peng, L. Ma, H. Chang, L. Chen, C. Liu, J. Xu, J. Li, N. Yan, Catal. Sci. Technol. 2 (2012) 915–917.
[42] F. Liu, Y. Yu, H. He, Chem. Commun. 50 (2014) 8445–8463.
[43] Z. Wu, B. Jiang, Y. Liu, H. Wang, R. Jin, Environ. Sci. Technol. 41 (2007) 5812–5817.
[44] T. Gu, R. Jin, Y. Liu, H. Liu, X. Weng, Z. Wu, Appl. Catal. B: Environ. 129 (2013) 30–38.
[45] C. Fang, D. Zhang, L. Shi, R. Gao, H. Li, L. Ye, J. Zhang, Catal. Sci. Technol. 3 (2013) 803–811.
[46] K. Hadjiivanov, Catal. Rev. Sci. Eng. 42 (2000) 71–144.
[47] E. Hums, Catal. Today 42 (1998) 25–35.
[48] R. Khodayari, C. Odenbrand, Ind. Eng. Chem. Res. 37 (1998) 1196–1202.
[49] B. Thirupathi, P. Smirniotis, J. Catal. 288 (2012) 74–83.
[50] H. Chang, J. Li, X. Chen, L. Ma, S. Yang, J. Schwank, J. Hao, Catal. Commun. 27 (2012) 54–57.
[51] A. Negreira, J. Wilcox, J. Phys. Chem. C 117 (2013) 24397–24406.